2015

Sequence Optimization at Signalized Diamond Interchanges Using High-Resolution Event-Based Data

Alexander M. Hainen
University of Alabama, ahainen@ua.edu

Howell Li
Purdue University, howell-li@purdue.edu

Amanda L. Stevens
Indiana Department of Transportation, amilynn1107@yahoo.com

Christopher M. Day
Purdue University, cmday@purdue.edu

Jim Sturdevant
INDOT, jsturdevant@indot.in.gov

See next page for additional authors

Authors
Alexander M. Hainen, Howell Li, Amanda L. Stevens, Christopher M. Day, Jim Sturdevant, and Darcy M. Bullock

Sequence Optimization at Signalized Diamond Interchanges Using High-Resolution Event-Based Data

Alexander M. Hainen
University of Alabama
P.O. Box 870205, Tuscaloosa, AL 35487-0205
Phone: 231-883-2669 Fax: 205-348-6862
Email: ahainen@ua.edu

Howell Li
Purdue University
550 Stadium Mall Drive, West Lafayette, IN 47907-2051
Phone: 765-496-7314 Fax: 765-494-0395
Email: howell-li@purdue.edu

Amanda L. Stevens
Indiana Department of Transportation
8620 East 21st Street, Indianapolis, IN 46219
Phone: 317-796-2661 Fax: 317-898-0897
Email: astevens@indot.in.gov

Christopher M. Day
Purdue University
550 Stadium Mall Drive, West Lafayette, IN 47907-2051
Phone: 765-494-9601 Fax: 765-494-0395
Email: cmday@purdue.edu

James R. Sturdevant
Indiana Department of Transportation
8620 East 21st Street, Indianapolis, IN 46219
Phone: 317-796-2661 Fax: 317-898-0897
Email: jsturdevant@indot.in.gov

Corresponding author:
Darcy M. Bullock
Purdue University
550 Stadium Mall Drive, West Lafayette, IN 47907-2051
Phone: 765-496-2226 Fax: 765-494-0395
Email: darcy@purdue.edu

November 14, 2014 TRB Paper **15-0644**

Word Count: 4,427 words + 12 x 250 words/Figure-Table = 4,427 + 3,000 = **7,427**

ABSTRACT
Signalized diamond interchanges are pairs of ramp intersections characterized by interlocked left turns and relatively close spacing. This paper describes a series of performance measures derived from high-resolution signal controller event data that can be used to optimize the internal phase sequence and offset to improve traffic flows within diamond interchanges and to qualitatively and quantitatively assess the progression of the interior movements. The new heuristic developed in this paper improves on traditional green band optimization techniques by incorporating actual demand profiles measured in the field. A field analysis was performed on a diamond interchange at I-69 and 96th Street in northwest Indianapolis, IN, where the existing sequence data was collected and used to model the alternative sequences to identify the optimal sequence. Interior operations were improved under the optimized settings: the percent of vehicle arrivals on green increased by 19% during the 0900-1500 midday plan. Video observations were used to corroborate the data and are included in a video synthesis of the time-space trajectories.

INTRODUCTION

Signalized diamond interchanges are pairs of ramp intersections characterized by interlocked left turns and relatively close spacing. The interlocked left turns at a diamond interchange can experience problems when interior queues back up through the interchange and block other movements. If this occurs, the entire interchange can become gridlocked. Diamond interchanges are characterized by four external entry points (origins) and four external exit points (destinations) (1) (2). To effectively operate a diamond interchange, it is critical to examine the external origin-destination paths and evaluate their impact on the interior storage and progression. Indiana has 161 signalized interchanges across the state which equates to over 8,000 signalized interchanges nationally.

There are four primary parameters in diamond interchange signal timing:

(i) *Splits*, which are set based on demand and made flexible with actuation,
(ii) *Cycle length*, which is usually a function of the adjacent intersections or crossing corridor,
(iii) *Offset*, which determines the relative schedule of signal timing at the two intersections (3), and
(iv) *Sequence* (order in which phases are served), which is often set arbitrarily by models, and which there is some interplay with the offset.

Previous studies of diamond interchange operation have focused on determining optimal splits, cycle length, and offset, or consider new timing schemes based on special assignments of movements to phases. However, the impact of the *sequence* of these phases (that is, whether the left turns lead or lag the thru movements) has not been studied to date. Since a sequence swap relocates a block of time, it is possible that one sequence might produce superior operation compared to another (under the appropriate offset). Passer III has historically been the most robust tool for designing diamond phase sequence, but has been designed for off-line operation using turning movement count data. This paper builds upon that concept and explores using a similar methodology based on high resolution controller event data for sequence and offset optimization at a diamond interchange. The advantage of using high resolution data is the ability to use field detection to directly measure the vehicle arrival characteristics.

LITERATURE BACKGROUND

Interchanges allow access to a freeway (access controlled roadway) from an arterial cross street. Most early interchanges were constructed as cloverleaf interchanges where the land could be acquired, or as yield-controlled diamonds. The original 1950 Highway Capacity Manual (HCM) recommended keeping the ramps widely separated and to utilize weaving sections (4). As volumes increased, it became necessary to signalize the interchanges (5) and the yield controlled diamonds naturally became signalized diamond interchanges (6). Pinell and Capelle identified two early operational functions of signals at diamond interchanges (7):

A. Separate all high-volume conflicting movements in the interchange area.
B. Minimize storing of vehicles between the two intersections.

Item B is particularly important. When a diamond interchange becomes gridlocked, queues on the ramps can back up onto the freeway, creating a dangerous situation where vehicles are slowing and stopping in high speed travel lanes. Early signal timing plans with mechanical

controllers were interval based (8) and rather complex (9), especially when conditional service based on actuation and pedestrian intervals are considered (10).

As computer-based controllers were implemented in the 1980's (11), actuated traffic control systems were used at diamond interchanges (1) and new phasing schemes commonly referred to as TTI 3-phase and TTI 4-phase were developed. Diamond-specific controllers and custom software were developed to make the traffic engineer's job less confusing (12) and to help allocate green time with better detection practices (13), especially during the peak periods and times when the flow had an imbalance (14).

In 1988, Fambro and Bonneson looked at the optimization and evaluation of diamond interchange signal timing and outlined the following optimization constraints (2):

A. Check that there is no spillback from one of the ramp intersections through the other intersection or from a left-turn lane back into a thru lane. If either condition occurs, gridlock may occur and the control strategy is unacceptable.
B. Check that the queue of vehicles on the off-ramp does not back onto the freeway. If so, the control strategy is probably not acceptable.
C. Check that individual movements are not delayed disproportionately to one another. If so, the green splits need adjustment and/or geometric modifications are required.
D. Check that the overall level of service at the interchange is within acceptable limits. If not, cycle length, phasing sequence, controller type and/or geometric modifications may be appropriate.

Item A is consistent with Pinnell and Cappelle's Item B (previously listed). Item B in Fambro and Bonneson's list is consistent with the higher level network goals. Item C and Item D are newer, performance measure based operational objectives. Stopped delay was a metric used by the authors to evaluate the performance and select offsets. In other studies, microsimulation (15) was used within hardware-in-the-loop (16) or software-in-the-loop (17) configurations to assess total delay (18), cycle length (19), actuation (20), and coordination with adjacent 8-phase intersections (21).

More recently, Englebrecht and Barnes explained single-controller diamond phasing nomenclature using a separate ring for each ramp intersection (22). An offset between the two rings (or *ring displacement*) was required for this to be implemented (which is a feature that still varies by traffic controller manufacturer). The offset is a function of the travel time and sequence used at the interchange.

There are three commonly used modeling/software packages used in the U.S. to analyze diamond interchange performance: (i) Passer III and (ii) the Highway Capacity Manual (or Highway Capacity Software) and (iii) Synchro. The Texas model and TRANSYT7F are also used on a lesser basis.

The latest version of Passer III was released in 1998. The software considers different timing strategies (traditional 3-phase, TTI 4-phase), left-turn treatments (protected, permitted, protected-permitted), and left-turn sequencing based on aggregated design volumes and intersection spacing and provides a recommended timing plan based on a number of performance metrics (23).

The Highway Capacity Manual (24) and Synchro provides an analysis methodology based on volumes, cycle length, and green times (which are determined by the splits) to estimate a delay that is used as a basis for determining the level of service. The approach can be used to

develop a timing plan by minimizing average delay. However, the HCM analysis does not itself provide a basis for optimizing the sequence and the offset.

MOTIVATION

The motivation of this paper is to provide practitioners with a way to identify the best sequence and offset combination by leveraging high-resolution event-based data to model the other three left-turn sequences. Event-based data that records every event at a signalized intersection can easily be collected from any modern traffic controller without additional equipment. Using event-based data will preserve field operation characteristics instead of using aggregated count and assuming a demand distribution. Previous work using event-based data at diamond interchanges allowed practitioners to easily and robustly identify the optimal offset by simulating offset changes (3), but only for the existing sequence. This paper expands that concept by modeling the other left turn sequences based on resorting the signal data and detection data.

STUDY INTERCHANGE

The diamond interchange at I-69 and 96th Street in Indianapolis was selected as the study location (Figure 1a). The diamond's interior left-turns are protected and the cycle length was 94 seconds. Figure 1b shows the boundaries of agency jurisdictions along 96th Street. The adjacent intersections are not coordinated with the diamond interchange and consequently starvation and atypical arrival patterns sometimes occur. This study focuses on operations in the interior of the diamond (between intersections 2 and 3). Figure 2a shows the phasing and detector layout for the interchange. The interchange is operated by two coordinated controllers, but the phasing nomenclature for a single controller is maintained. The southbound ramp included the following phases (Ø):

- Ø1: Westbound Left (internal approach to freeway on-ramp)
- Ø2: Eastbound Thru (external approach)
- Ø3: Southbound Left & Right (exit ramp approach)
- Overlap-F (parents Ø1, Ø2): Westbound Thru (internal approach).

Similarly, the northbound ramp includes the following phases:

- Ø5: Eastbound Left (internal approach to freeway on-ramp)
- Ø6: Westbound Thru (external approach)
- Ø7: Northbound Left & Right (exit ramp approach)
- Overlap-B (parents Ø5 and Ø6): Eastbound Thru (internal approach).

Figure 2b-d show the four possible sequences for the interchange, noting that the ring displacement is the difference between the start of the coordinated phases in each ring (indicated by an asterisk). Ø2 and Ø6 are coordinated, while Ø1 and Ø5 operate left turns. Figure 2b shows the existing "lag-lead" sequence where Ø1 lags Ø2, and Ø5 leads Ø6. For optimal interchange performance, a traffic engineer must select (1) the most effective sequence (lead-lead, lead-lag, lag-lead, lag-lag) and then (2) the most effective offset (which varies with sequence). In this study, conditions during the weekday midday timing plan (0900-1500) were considered.

MEASURES OF EFFECTIVENESS

Arrivals on green (AOG) and delay were used to evaluate sequence and offset combinations. Both of the controllers at the interchange featured high-resolution event-based data loggers (25) capable of logging events to the nearest tenth of a second. The events of interest included (i) the phases at each intersection and (ii) the interior advance detection events. These pieces of information are used to construct Purdue Coordination Diagrams (PCDs) and assess AOG and delay (26). Figure 3 shows the basics of a PCD for three cycles of a single westbound thru lane where the stop bar arrivals are plotted in relationship to the green or red signal status. The light gray markers are the original detection events (occurring when the vehicle is approximately 9 seconds upstream from the stop bar), the red markers are estimated arrival at back of queue, the green markers are the estimated shockwave propagation when the vehicles in the queue start to move (based 2-second departure headways), and the black markers are when the vehicles cross the stop bar.

Consider the following example observations in the third cycle of Figure 3. The first car to queue crossed the advance detector (callout "i"), arrived at the stop bar on *red* 9 seconds later (callout "ii"), and crossed the stop bar after 25 seconds of delay (callout "iii") at the start of green (callout "iv"). The last car to queue crossed the advance detector (callout "v") and reached the back of standing 5-car queue 7 seconds later which constitutes an arrival on *red* (callout "vi"), started to roll again after 7 seconds of delay (callout "vii"), and finally crossed the stop bar 2 seconds later (callout "viii"). At this point, the queue has cleared and the next car that crossed the advance detector (callout "ix") was able to cleanly proceed through the interior and arrived at the stop bar on *green* (callout "x") with no delay.

The PCD examines how vehicles arrive downstream at the stop bar, but the same data can be linked with the upstream signal to associate vehicles with their origin. Figure 4 shows simplified time space diagrams for each of the sequences. The detections (diamond symbols) for eastbound thru vehicles (Figure 4a) and westbound thru vehicles (Figure 4c) are used to estimate linear trajectories tracing the vehicles from an origin phase to their destination by adding or subtracting the travel time in either direction. For example, callout "i" shows three westbound vehicles that most likely originated from the ramp movement (Ø7). This information is important in the next step when other sequences are simulated.

MODELLING ALTERNATIVE SEQUENCES USING HIGH RESOLUTION DATA

A technique was developed to predict intersection conditions under a sequence swap. When a swap occurs, it affects two things: (1) the platoons leaving that intersection, and thus the arrival profile at the downstream intersection, and (2) the served green at that intersection, especially with overlaps when the parent phases are rearranged. There are three different sequences to be evaluated based on the simulated swaps:

1. The first simulation is an existing-swapped arrangement which would be lag-lag. This sequence is shown is Figure 4e. The simulated lag-lead eastbound trajectories are shown in Figure 4d and the simulated westbound trajectories are shown in Figure 4f.
2. The second simulation is a swapped-existing arrangement which would be lead-lead. This sequence is shown is Figure 4h. The simulated lag-lead eastbound trajectories are shown in Figure 4g and the simulated westbound trajectories are shown in Figure 4i.
3. The third simulation is swapped-swapped arrangement which would be lead-lag. This sequence is shown is Figure 4k. The simulated lag-lead eastbound trajectories are shown in Figure 4j and the simulated westbound trajectories are shown in Figure 4l.

The detection times as observed with the existing sequence are moved accordingly by the same amount of time that their origin phase is moved (the phase from which the vehicle detections originated). For example, Figure 4e illustrates predicted conditions under lag-lag (existing-swapped) phasing. The southbound ramp maintains the existing lagging left while the northbound ramp changes from lead to lag, which is modeled by swapping events associated with Ø5 and Ø7. In Figure 4f, Ø5 and Ø7 change the order in which they occur. To model the impact of this change, the vehicles departing from Ø7 are shifted. Note the movement of the platoon departing from Ø7 (Figure 4f, callout "ii"; compare with Figure 4c, callout "i"). Interestingly, in Figure 4c, these vehicles arrive on red at the downstream intersection (during Ø4), but in Figure 4f, after the sequence swap, they are expected to arrive on green (during Ø2).

The same evaluation can be done for a swap at the other intersection. In Figure 4a, callout "iii" shows an eastbound platoon originating from Ø4 that arrives on green at the downstream intersection during Ø5. Figure 4h shows a lead-lead (swapped-existing) configuration that changes the sequence of Ø1 and Ø4. This is reflected by the swapping of the green times of those phases in Figure 4g, as well as the movement of the platoon originating from Ø4 (Figure 4g, callout "iv").

Figure 4 characterizes each of the four sequences for thru movements. The interior left turn movements can be analyzed similarly by relating detections in the left turn lanes with the states of the left turn phases. A final note about the swappable pair method is that a single swappable phase (non-coordinated movement) without a companion swappable phase will not be moved. This is an advantage of this heuristic in that it can account for skipped phases based on the actual measured demand.

OFFSET OPTIMIZATION

Having developed a model to predict conditions under a new sequence, it is now possible to optimize offsets under the four alternative sequences to determine which sequence provides the best interchange performance. In a previous study, conditions under an offset change were simulated by temporally displacing vehicle detections and phase times and recalculating the MOEs (3). Delay and arrivals on green (AOG) were calculated for all possible offsets under the four different sequences. Figure 5 shows how these performance measures vary with offset adjustments under the existing sequence. Figure 5a,c,e,g show how AOG varies with offset for each of the four internal movements, while Figure 5i shows the comprehensive results for the interchange. Callout "i" identifies the optimal adjustment for maximum AOG. Similarly, Figure 5b,d,f,h,j repeat this analysis for delay. Callout "ii" identifies the optimal offset for minimum delay. The two optimal offset adjustments are roughly the same

Figure 6 repeats this analysis for all of the different possible sequences. Figure 6a repeats the same overall results for the existing sequence. Figure 6b-d show the results of the offset sweep (sequentially stepping through the domain of offsets) carried out under predicted conditions under the alternative sequences. The callouts highlight the optimal offset adjustments in each graphic.

For example, if the lag-lag sequence was selected (Figure 6b), callout "ii" suggests that between 8 and 13 seconds should be added to the existing offset in the controller. However, the maximum AOG of 15,116 is less than the value of 16,427, and the total delay of 43 hours is greater than the value of 41 hours under the existing sequence (Figure 6a). Because the optimal conditions under lag-lag are worse than the optimal conditions under the existing sequence (lag-lead), lag-lag would not be selected as an alternative sequence. Figure 6c shows the same curves

for the lead-lead sequence and Figure 6d shows the same curves for the lead-lag sequence. Their optimal offset adjustments are identified by callouts "iii" and "iv" respectively.

The four sets of performance measure curves are synthesized to identify the best performing sequence and offset adjustment. Figure 7a-d show curves that represent the results of offset sweeps for the four possible alternative sequences. In each graph, AOG is plotted on the X-axis and delay is plotted on the Y-axis. Figure 7a, callout "i" shows the optimal offset under the existing sequence (lag-lead). The red square shows this data point in each graph, while the yellow triangle shows the global optimum for all sequences. Figure 7e shows all four offset sweeps superimposed, which clearly shows the optimal condition. The lead-lead sequence achieved the lowest delay and highest AOG (Figure 7e, callout "ii"). Based on this analysis, the lead-lead sequence and the optimal offset were implemented at the interchange.

VISUALIZATION AND OUTCOME ASSESSMENT

The lead-lead sequence and optimized offset were implemented on December 5, 2013. Field observations confirmed improved performance in all directions and is documented in the following sections.

Improved Signal Coordination

The PCDs for the westbound thru movement (Figure 8) show considerable improvement in AOG. Under the existing sequence, vehicles from the upstream ramp arrived before the start of green (callout "i") and vehicles from the upstream thru arrived late in the green (callout "ii") and were clipped by the end of green (callout "iii"). After the lead-lead sequence and optimal offset were implemented, the PCD (Figure 8b) showed much cleaner progression, with 94.0% of vehicles arriving on green. Vehicles from the upstream thru (callout "v") arrived nicely at the start of green and the platoons of vehicles from the upstream ramp (callout "iv") also arrived during green.

Validation of the Prediction Methodology

Flow profile diagrams are used in Figure 9 and Figure 10 to illustrate conditions at the interchange before adjustment; from a prediction of the impact of the new timing; and after the adjustments were actually implemented. Figure 9 shows that with the existing lag-lead sequence (Figure 9c and Figure 9d), the westbound thru vehicles (Figure 9c) from the upstream ramp arrived before the start of the thru green (callout "i") and westbound left vehicles (Figure 9d) from the upstream thru arrived before the start of the left turn green (callout "ii"). The predicted profiles (Figure 9e and Figure 9f) closely matched the post-adjustment profiles, where the westbound thru vehicles (Figure 9g) arrived during green (callout "iii") and the westbound left turn vehicles (Figure 9h) also arrived during green (callout "iv").

Similar improvements occurred in the eastbound direction (Figure 10). Under the existing sequence, the eastbound thru vehicles (Figure 10c) from the upstream ramp movement arrived during Ø5 (callout "i"). Under this scheme, the left turn was sequenced to occur after the entry of vehicles coming from the ramp—which was not a common usage, with few vehicles making freeway "U-turns" through the interchange. Consequently, the eastbound left vehicles (Figure 10d) which overwhelmingly originated from the upstream thru movement arrived just after Ø5 ended. These vehicles arrived on red, queued in the interior of the interchange, and experienced heavy delay (callout "ii"). After the new sequence was implemented, the predicted results (Figure 10e and Figure 10f) again closely matched the actual results in the field, where the eastbound thru vehicle (Figure 10g) saw nearly all vehicles arriving during the appropriate green

(callout "iii"), with the eastbound left vehicles (Figure 10h) arriving nicely within the left turn green band (callout "iv").

Figure 11a provides a better overview of how closely the modelled and actual arrival platoon profiles matched (the curves are nearly on top of one another). Figure 11a compares the platoon profiles arriving at the westbound thru from phase 7 (left pair of traces) and phase 6 (right pair of traces). The close alignment of the predicted with the actual validates the assumption that linear superposition can be used to model predicted phase sequence impact on the westbound thru movement. Similarly, Figure 11b, Figure 11c, and Figure 11d show strong empirical evidence that linear superposition is effective for modelling arrivals for westbound left, eastbound thru, and eastbound left, respectively.

Video Analysis

To further document this improvement, an annotated video with animated time-space diagrams capturing 100% arrivals on green for the westbound thru movement is shown in Figure 12 (27). The vehicles head from the left side of the screen (camera 1) and exit the diamond at the other side of the interchange (camera 2). The active northbound ramp phase at the origin on the time space is used to associate detections with their origin and the downstream southbound ramp phase at the destination is used to characterize arrival on green performance. The video records two cycles on December 6, 2013 after the implementation and shows excellent interior performance with high AOG, low delay, and no internal queuing or congestion.

CONCLUSIONS

Diamond interchanges are a common geometric grade separation between access controlled freeways and crossing arterial roads. Passer III has historically been the most robust tool for designing diamond phase sequence. This paper builds upon that concept by leveraging high-resolution event-based data for modelling alternative left-turn sequencing at signalized diamonds. The linear superposition techniques used to model arrival characteristics were validated by comparing predicted arrivals with actual arrivals (Figure 11). This modelling technique was demonstrated to be effective at identifying a new sequence and offset that resulted in quantifiable improvement in field operation. For the study diamond interchange at I-69 and 96th Street, the methodology in this paper increased the interior AOG by 19% for the 0900-1500 timing plan.

Traditionally, field tuning is the responsibility of the traffic engineer and validation is often limited to visual field inspection of operations for a few hours to tune offsets. Adjusting phase sequence in the field is a very difficult task to effectively accomplish, even for the most experienced traffic engineer. High resolution data makes it possible to monitor and assess all time of day plans, including times or days of the week when field visits may not be feasible. This methodology is practice ready and could even be incorporated into an adaptive algorithm. All modern traffic controllers provide this data source and the data could easily be extracted from the controller and analyzed as described in this paper. Future research will involve more consideration of the adjacent signals to better characterize the change in external arrival profiles.

ACKNOWLEDGEMENT

This work was supported in part by the Joint Transportation Research Program and Pooled Fund Study (TPF-5(258)) led by the Indiana Department of Transportation (INDOT) and supported by the state transportation agencies of California, Georgia, Kansas, Minnesota, Mississippi, New Hampshire, Texas, Utah, Wisconsin, and Pennsylvania, the Federal Highway Administration

Arterial Management Program, and the Chicago Department of Transportation. The contents of this paper reflect the views of the authors, who are responsible for the facts and the accuracy of the data presented herein, and do not necessarily reflect the official views or policies of the sponsoring organizations. These contents do not constitute a standard, specification, or regulation.

WORKS CITED

1. Messer CJ, Chang MS. Traffic Operations of Basic Actuated Traffic Control Systems as Diamond Interchanges. Transportation Research Record. 1987; 1114.
2. Fambro DB, Bonneson JA. Optimization and Evaluation of Diamond Interchange Signal Timing. In ITE 1988 Compendium of Technical Papers; 1988. p. 125-129.
3. Hainen AM, Stevens AL, Freije RS, Day CM, Sturdevant JR, Bullock DM. High-Resolution Event-Based Data at Diamond Interchanges: Performance Measures and Optimizing Ring Displacement. Transportation Research Record. 2015; Forthcoming.
4. The Committee on Highway Capacity. Highway Capacity Manual: Practical Applications of Research. Manual. Washington, D.C.: Traffic and Operations Highway Research Board, U.S. Department of Transportation; 1950.
5. Moskowitz K. Signalizing a Diamond Interchange. In Northwest Traffic Engineering Conference; 1959; Chicago. p. 87-99.
6. LeRoy HM, Clinton JW. Signalization of Diamond Interchanges. In ITE Proceedings; 1960; Washington, D.C. p. 196-202.
7. Pinnell C, Capelle DG. Design and Operations of Diamond Interchanges. In ; 1961; College Station.
8. Spitz S. Signalization of Diamond Interchanges. Traffic Engineering. 1964; 15-17: p. 15-17.
9. Hayes E. Programming a digital simulation model of a freeway diamond interchange. In A.C.M. National Proceedings; 1966. p. 117-129.
10. Munjal PK. An Analysis of Diamond Interchanges. Transportation Research Record. 1971; 349.
11. Leisch JP. Innovations of Diamond Interchanges in the Urban Environment. ITE Journal. 1985.
12. de Camp GB. A Primer on Diamond Interchanges. TexITE News. 1993: p. 3-13.
13. Herrick GC, Messer CJ. Strategies for Improving Traffic Operations at Oversaturated Diamond Interchanges. Report. College Station: Texas Department of Transportation, Texas Transportation Institute; 1992. Report No.: FHWA/TX-92/1148-4F.
14. Lum KM, Lee CE. Acutated Traffic Signal Control at Diamond Interchange. Journal of Transportation Engineering. 1992; 118(410-429).

15. Lee S, Messer CJ, Oh Y, Lee C. Assessment of Three Simulation Models for Diamond Interchange Analysis. Journal of Transportation Engineering. 2004; 104(304-312).

16. Koonce PJV, Urbanik II T, Bullock D. Evaluation of Diamond Interchange Signal Controller Settings by Using Hardware-in-the-Loop Simulation. Transportation Research Record. 1999; 1683.

17. Nelson EJ, Bullock D, Urbanik T. Implementing Actuated Control of Diamond Interchanges. Journal of Transportation Engineering. 2000;(390-395).

18. Xu H, Liu H, Tian Z. Control Delay at Signalized Diamond Interchanges Considering Internal Queue Spillback. Transportation Research Record. 2010;(123-132).

19. Kovvali VG, Messer CJ, Chaudhary NA, Chu CL. Program for Optimizing Diamond Interchanges in Oversaturated Conditions. Transportation Research Record. 2002; 1811(166-176).

20. Lee S, Messer CJ, Choi K. Actuated Signal Operations of Congested Diamond Interchanges. Journal of Transportation Engineering. 2006; 132(790-799).

21. Chaudhary NA, Chu CL. Guidelines for Timing and Coordinating Diamond Interchanges with Adjacent Traffic Signals. Report. College Station: Texas Department of Transportation, Texas Transportation Institute; 2000. Report No.: TX-00/4913-2.

22. Englebrecht RJ, Barnes KE. Advanced traffic Signal Control for Diamond Interchanges. Transportation Research Record. 2003;(2-25).

23. Venglar S, Koonce P, Urbanik II T. Passer III-98 Applications and User's Guide. Manual. College Station: Texas Department of Transportation, Texas Transportation Institute; 1998.

24. Transportation Research Board. Highway Capacity Manual. Manual. Washington, D.C.: National Academies, TRB; 2010.

25. Smaglik EJ, Sharma A, Bullock DM, Surdevant JR, Duncan G. Event-based data collection for generating actuated controller performance measures. Transportation Research Record. 2007; 2035.

26. Day CM, Haseman R, Premachandra H, Brennan Jr. TM, Wasson JS, Sturdevant JR, et al. Methodologies for Visualizing High-Resolution Event Data and Measuring Travel Time. Transportation Research Record. 2011 February; 2192(10.3141/2192-04).

27. Hainen AM, Li H, Stevens AL, Bullock DM. [Video].; 2014. Available from: http://dx.doi.org/10.4231/R7VD6WCH.

LIST OF FIGURES

a) Aerial map of Diamond Interchange

b) Network Diagram noting system jurisdiction

Figure 1 Map of I-69 / 96th Street Diamond showing adjacent intersections and agency jurisdictions

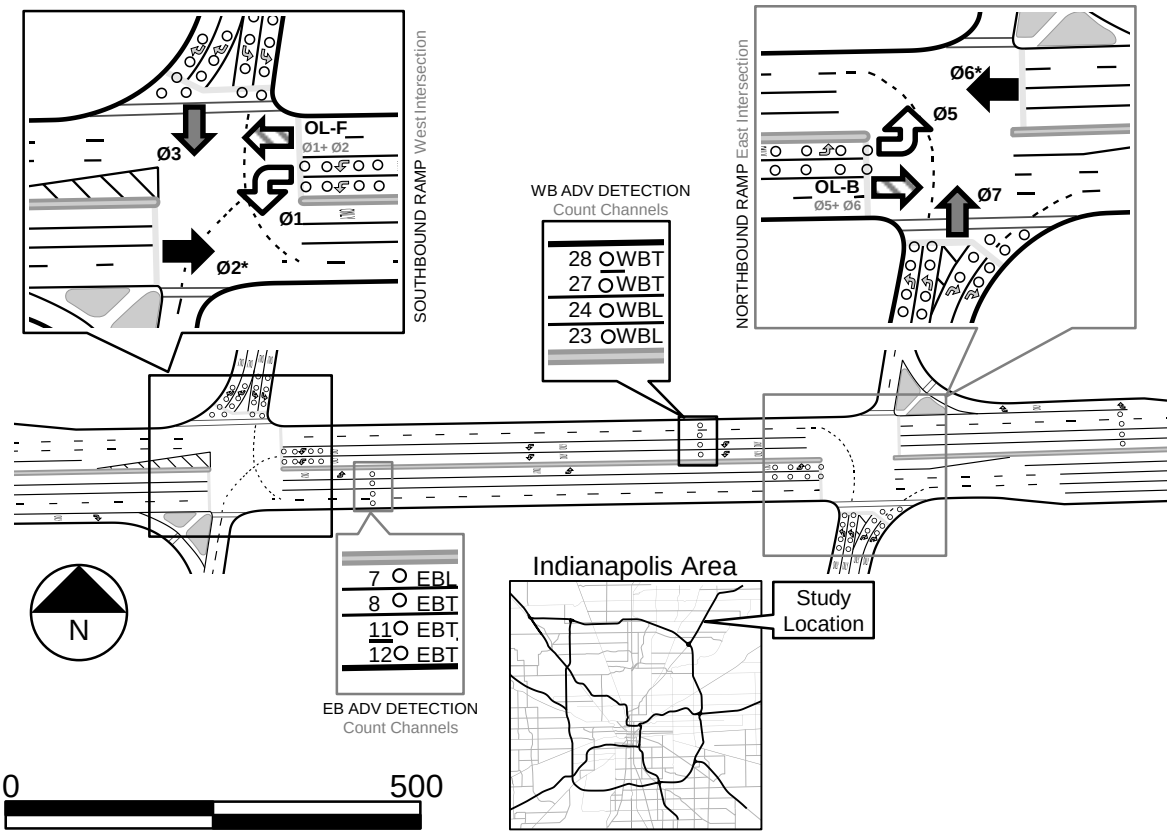

a) Phasing and Detection Maps

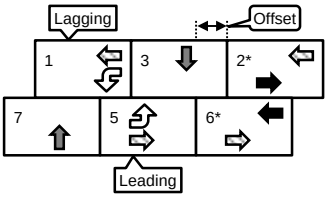

b) Lag-Lead Sequence (Existing)

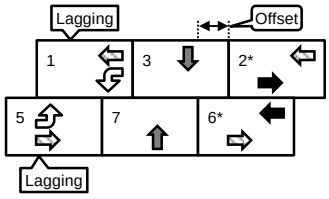

c) Lag-Lag Sequence

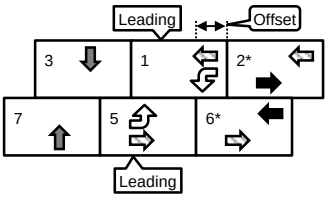

d) Lead-Lead Sequence

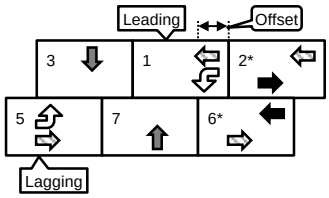

e) Lead-Lag Sequence

Figure 2 Map of Diamond Interchange at I-69 and 96th Street

**Indicates coordinated phase*

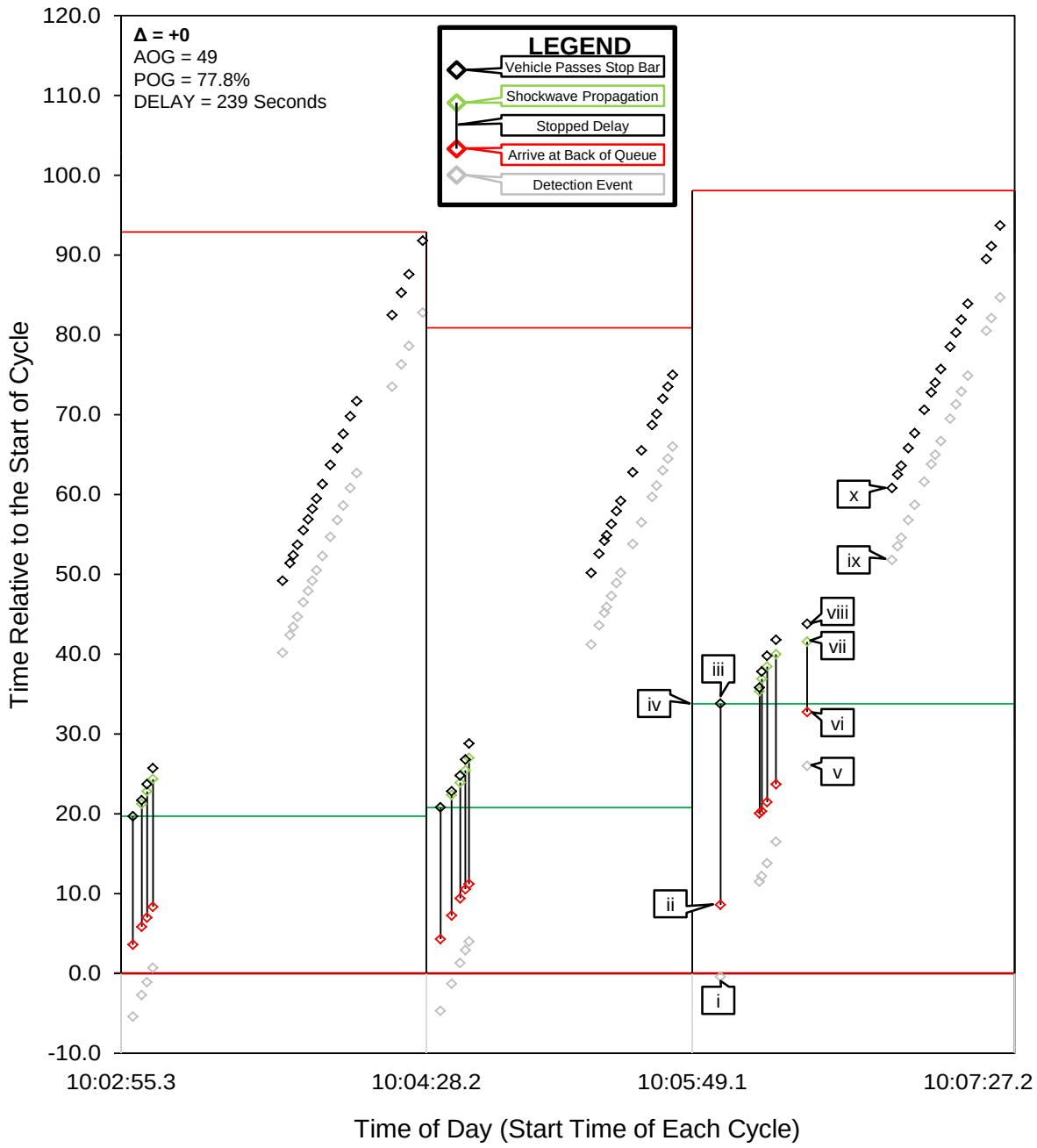

Figure 3 PCD Explanation of AOG and Delay Calculations

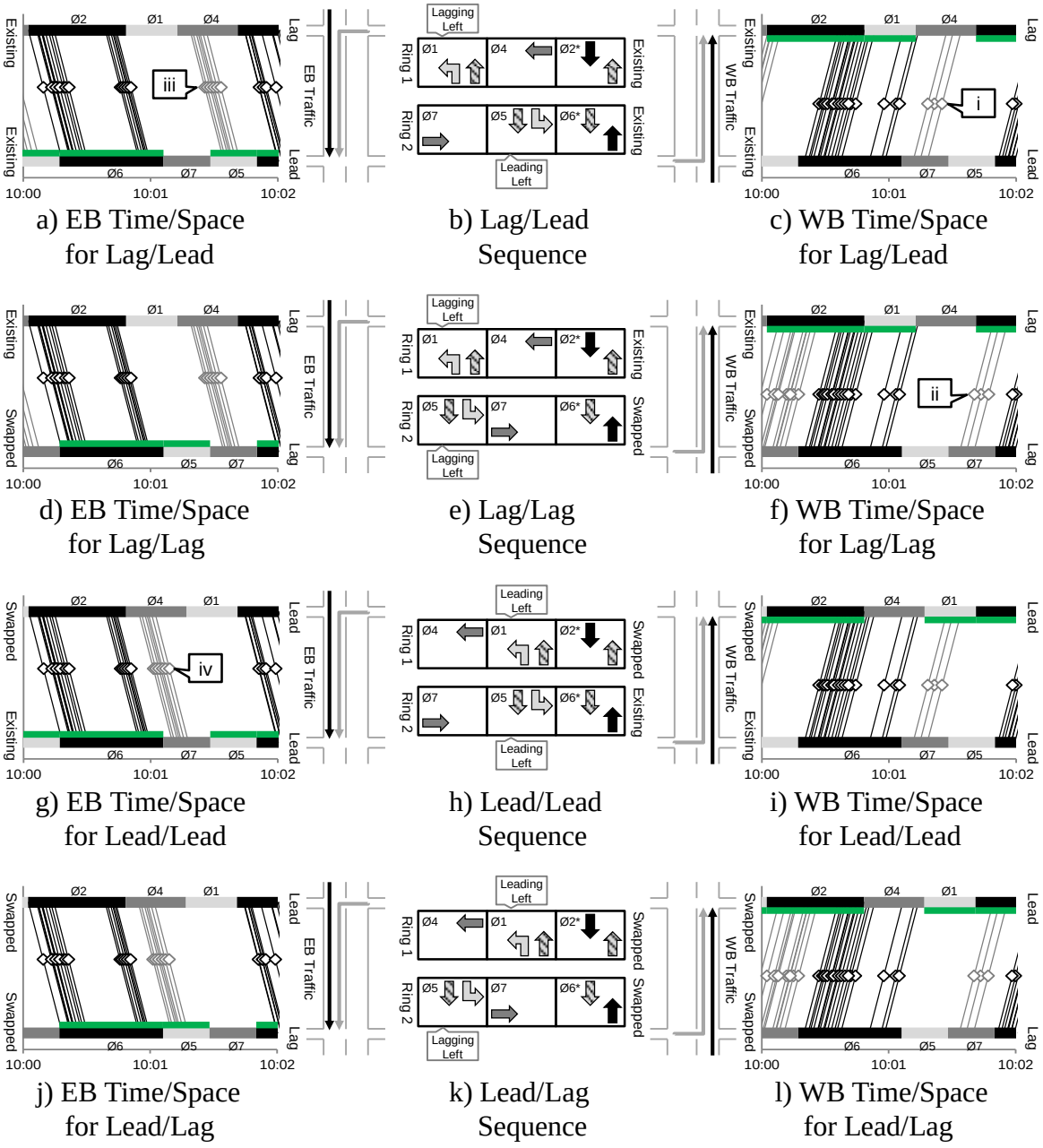

a) EB Time/Space for Lag/Lead

b) Lag/Lead Sequence

c) WB Time/Space for Lag/Lead

d) EB Time/Space for Lag/Lag

e) Lag/Lag Sequence

f) WB Time/Space for Lag/Lag

g) EB Time/Space for Lead/Lead

h) Lead/Lead Sequence

i) WB Time/Space for Lead/Lead

j) EB Time/Space for Lead/Lag

k) Lead/Lag Sequence

l) WB Time/Space for Lead/Lag

Figure 4 Sequence swap concept illustrated in time space diagrams and platoon shifting

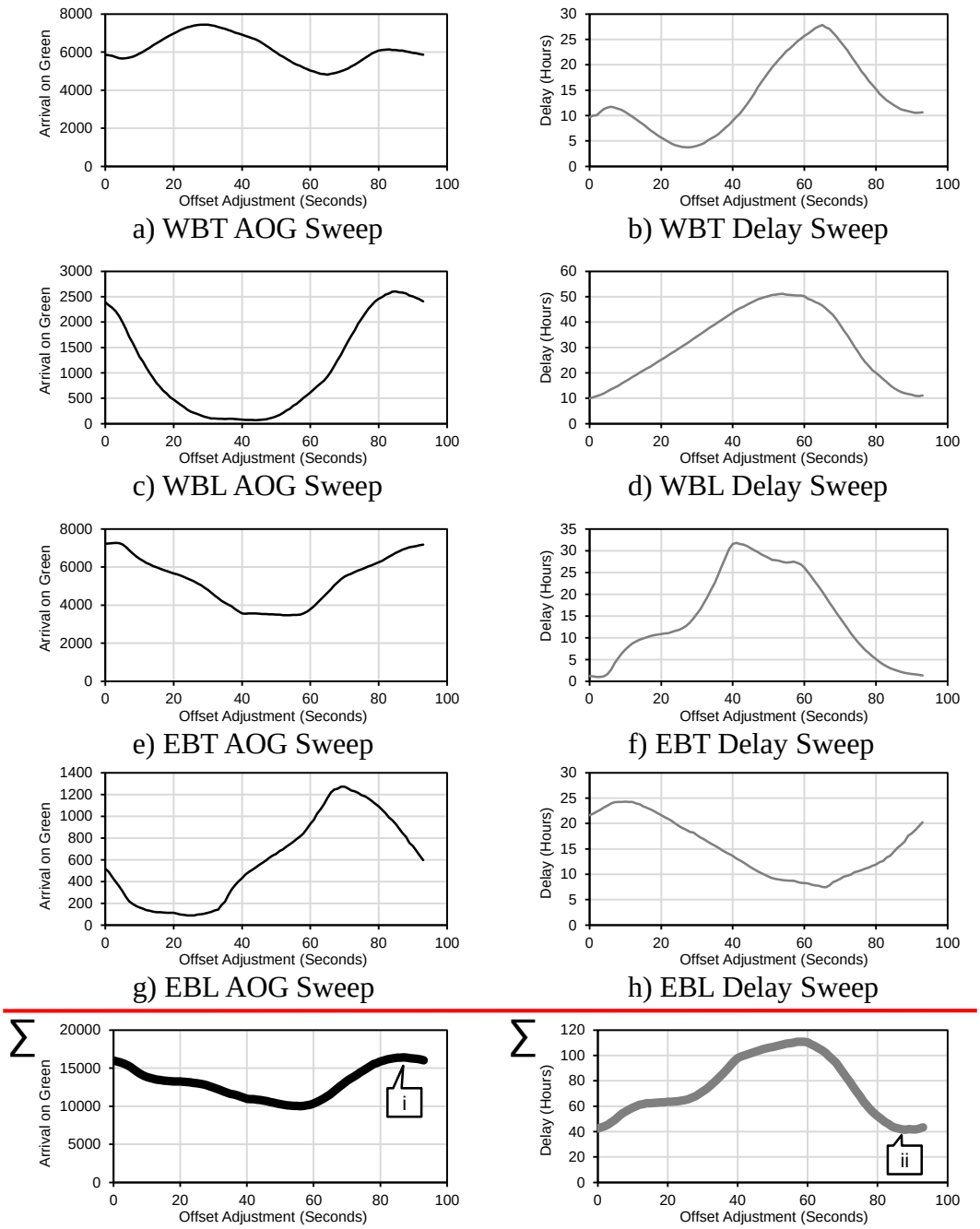

a) WBT AOG Sweep

b) WBT Delay Sweep

c) WBL AOG Sweep

d) WBL Delay Sweep

e) EBT AOG Sweep

f) EBT Delay Sweep

g) EBL AOG Sweep

h) EBL Delay Sweep

i) Lag-Lead Interchange AOG Sweep

j) Lag-Lead Interchange Delay Sweep

Figure 5 Offset sweep for lag-lead sequence broken down by movement

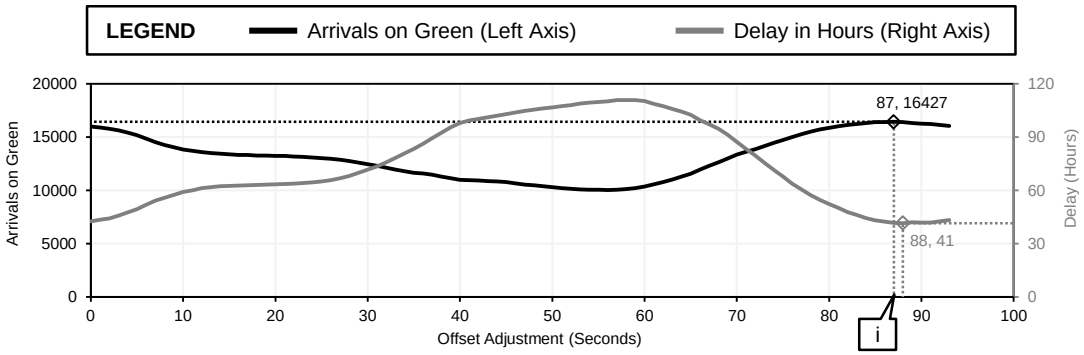

a) Lag-Lead Offset Performance Sweeps (Existing-Existing Sequence)

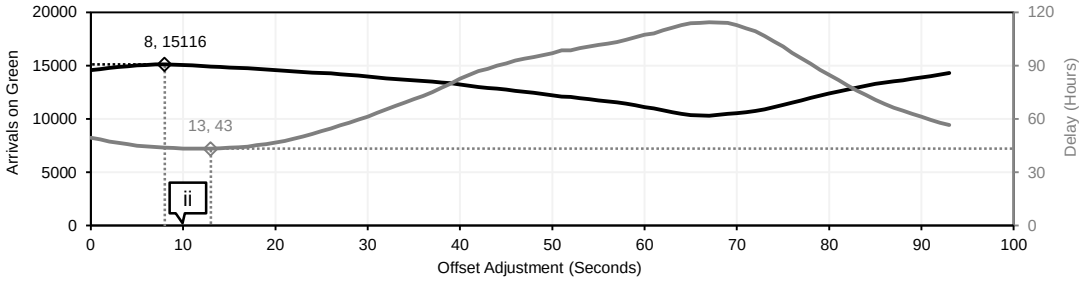

b) Lag-Lag Offset Performance Sweeps

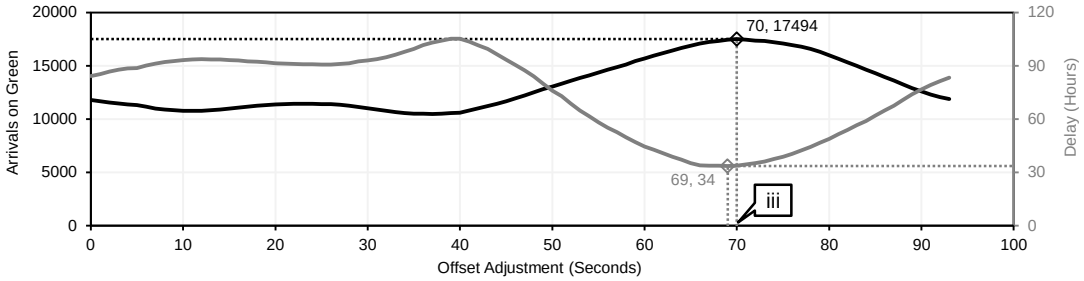

c) Lead-Lead Offset Performance Sweeps

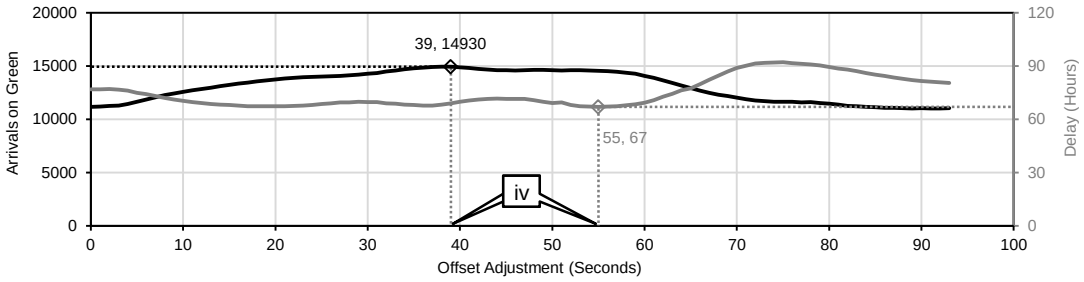

d) Lead-Lag Offset Performance Sweeps

Figure 6 Offset sweep for each of the four sequences

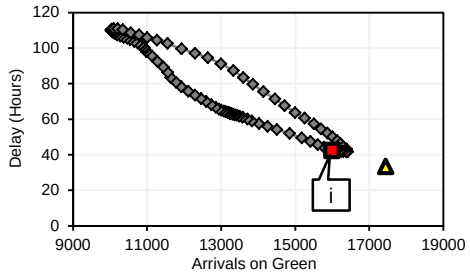

a) Lag-Lead Offset Performance Sweep

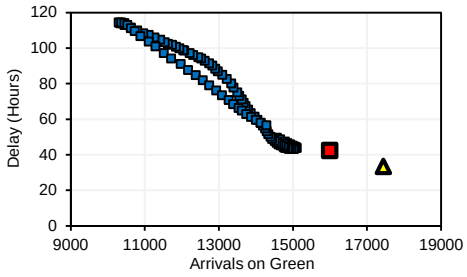

b) Lag-Lag Offset Performance Sweep

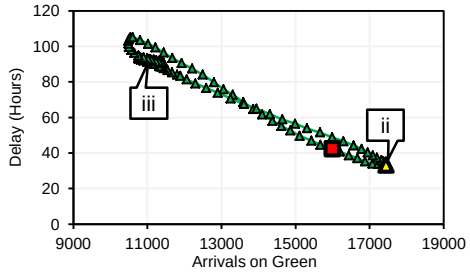

c) Lead-Lead Offset Performance Sweep

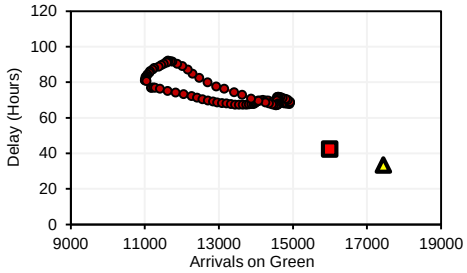

d) Lead-Lag Offset Performance Sweep

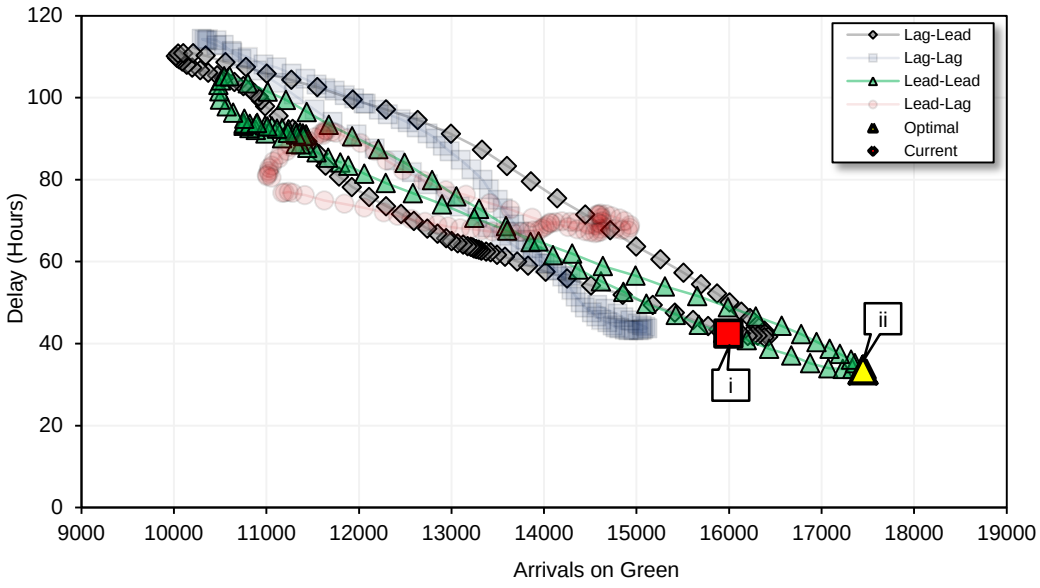

e) Offset Performance Sweeps for All Sequences

Figure 7 Solution space for each of the four sequences

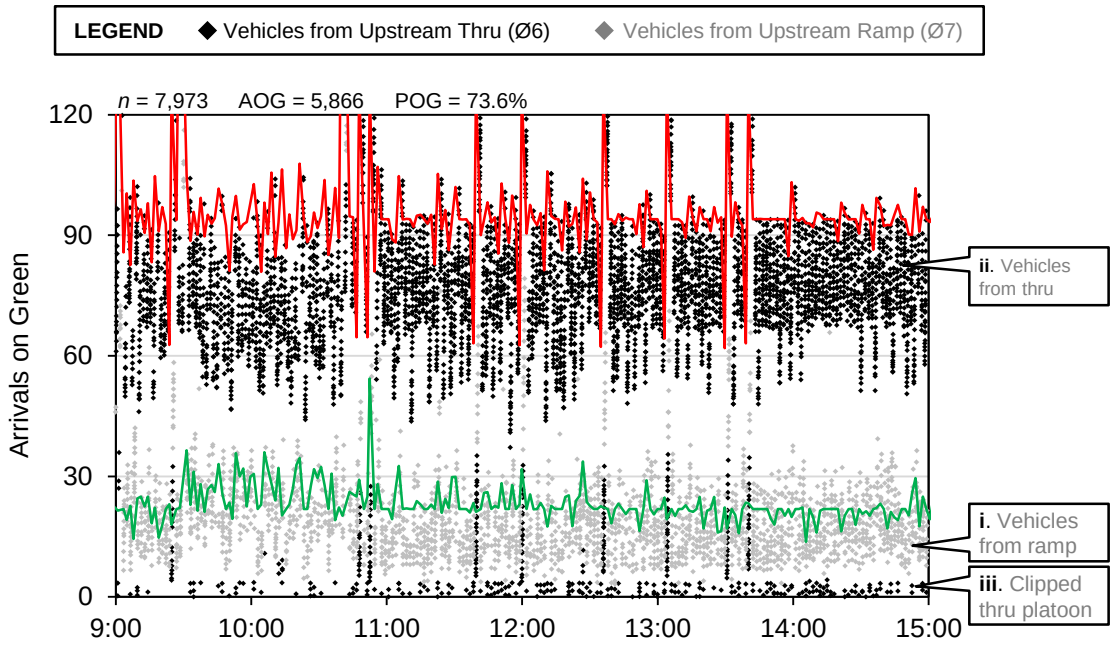

a) PCD showing lag-lead sequence (Before)

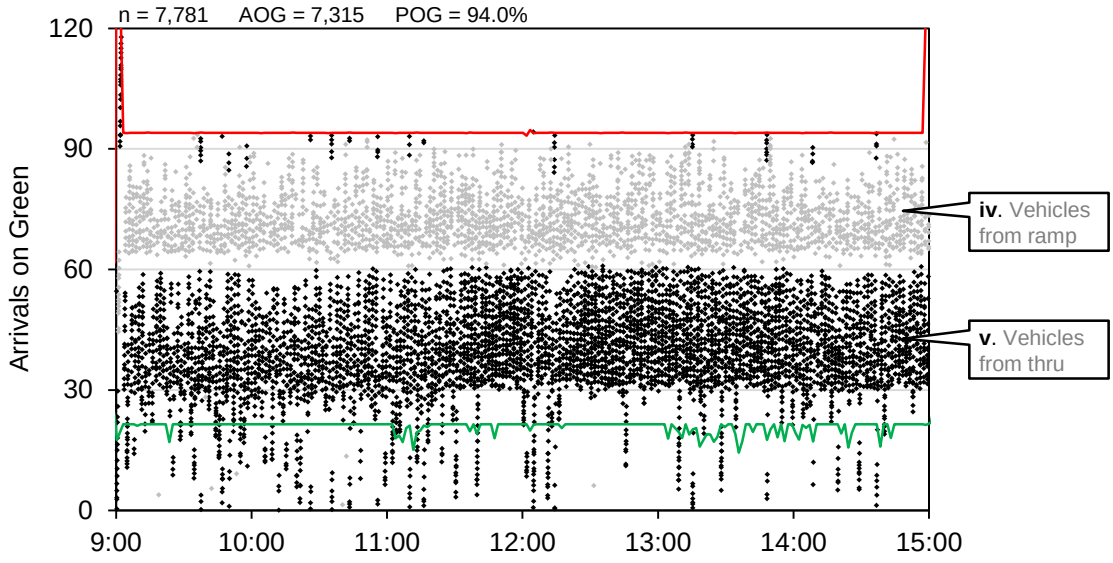

b) PCD showing Lead-Lead optimal sequence(After)

Figure 8 Westbound thru PCD showing before optimization (lag-lead sequence) and after optimization (lead-lead sequence implementation)

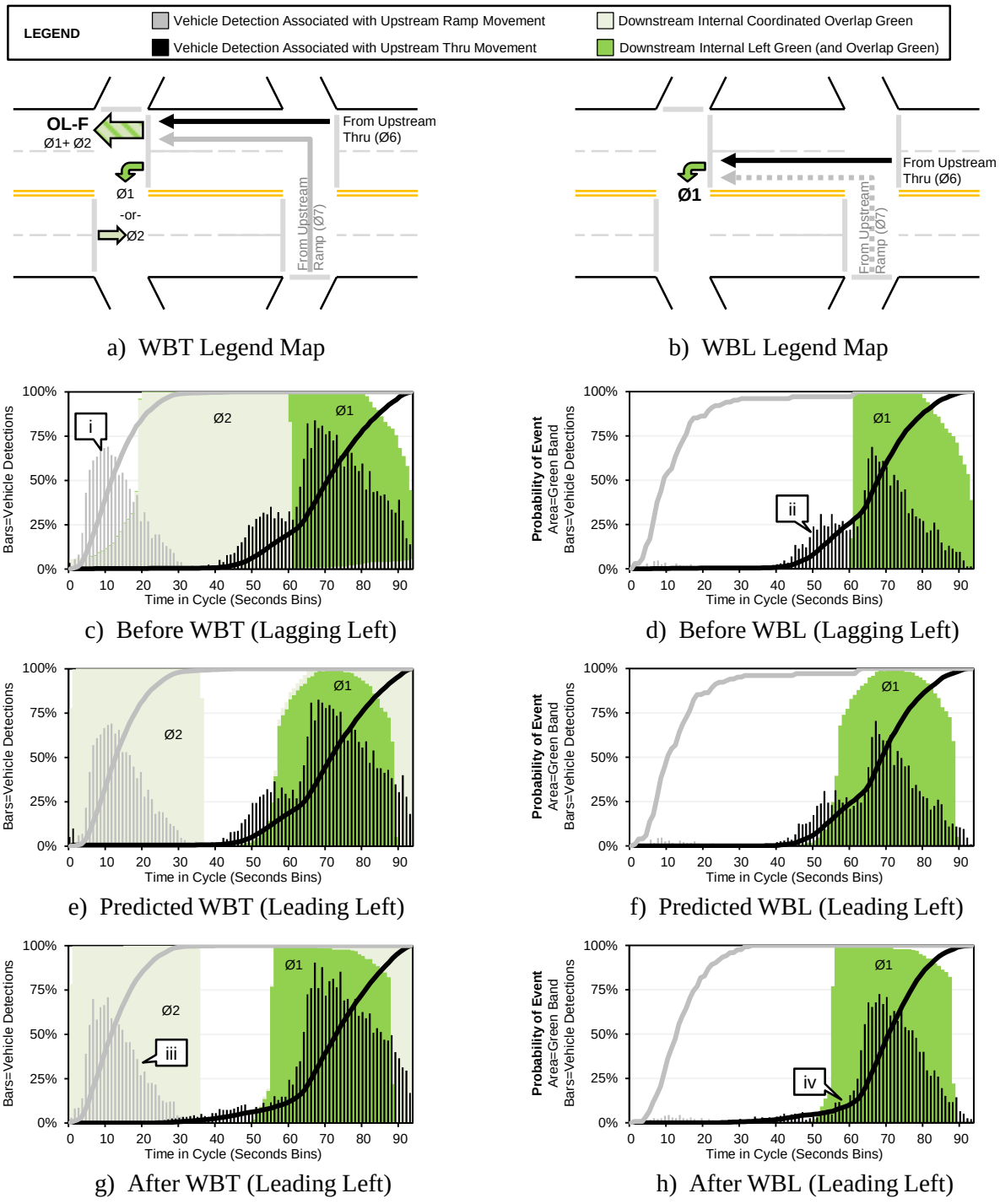

Figure 9 Flow profile analysis of model performance for the WB movements

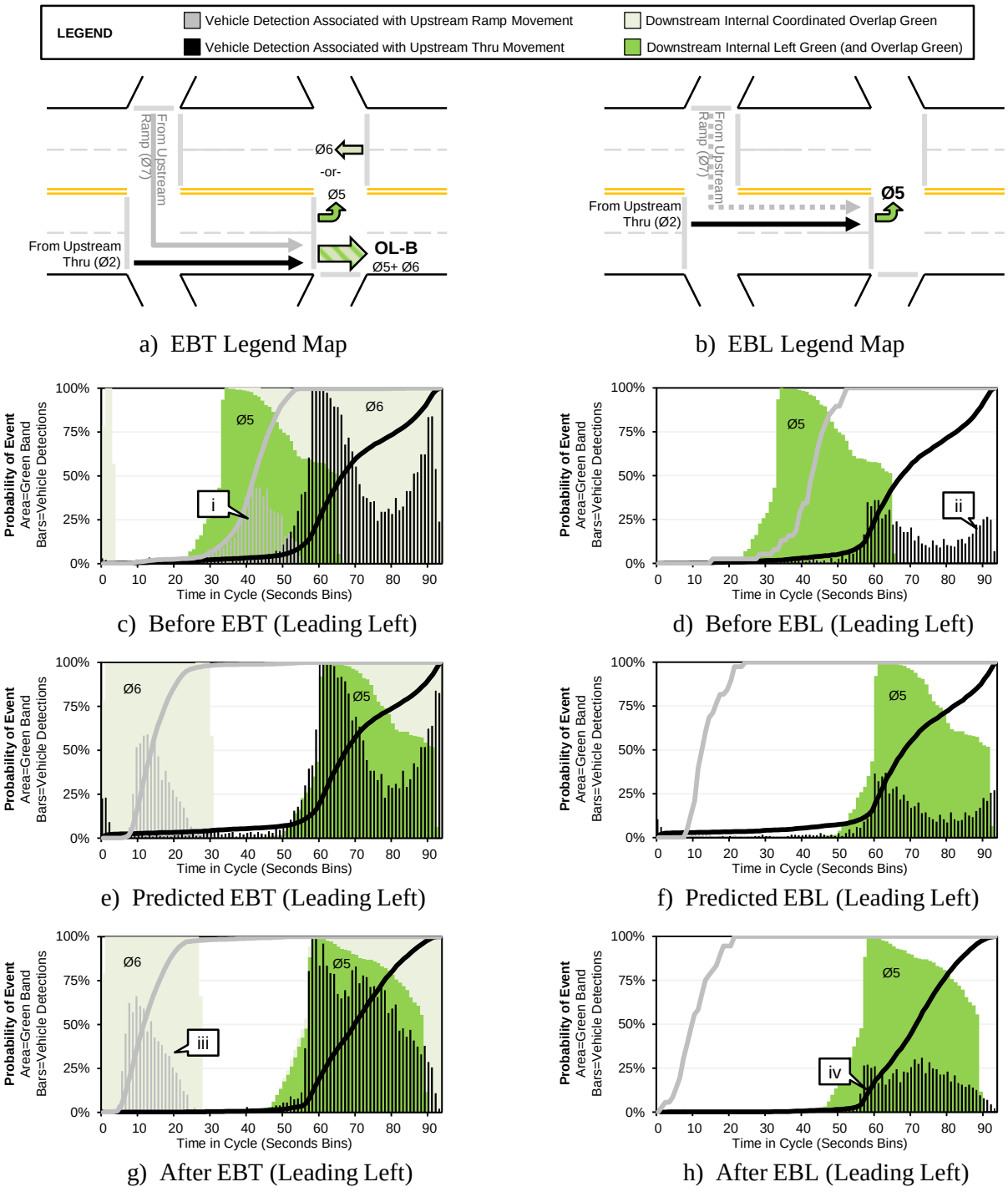

a) EBT Legend Map

b) EBL Legend Map

c) Before EBT (Leading Left)

d) Before EBL (Leading Left)

e) Predicted EBT (Leading Left)

f) Predicted EBL (Leading Left)

g) After EBT (Leading Left)

h) After EBL (Leading Left)

Figure 10 Flow profile analysis of model performance for the EB movements

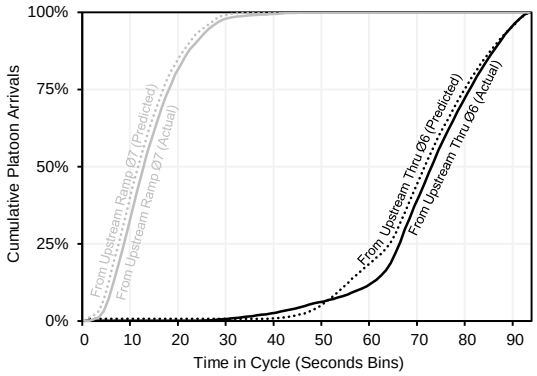

a) WBT Predicted vs. Actual

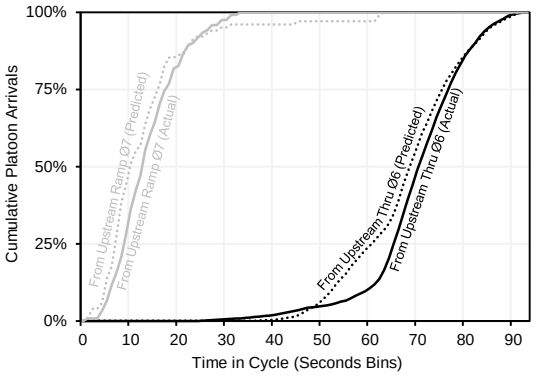

b) WBL Predicted vs. Actual

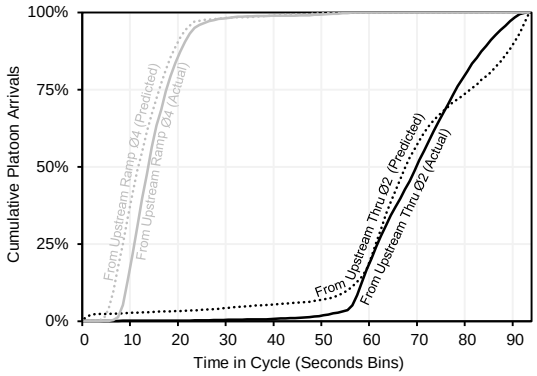

c) EBT Predicted vs. Actual

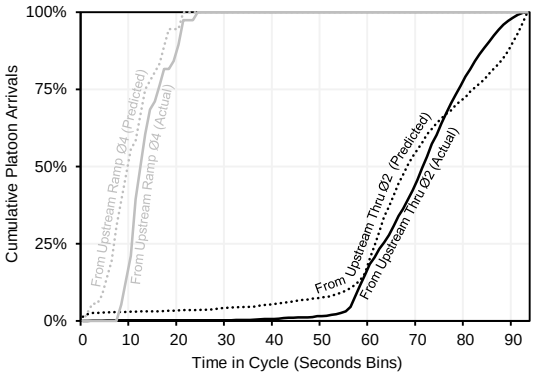

d) EBL Predicted vs. Actual

Figure 11 Direct Comparison of Predicted vs. Actual Cumulative Platoon Arrivals

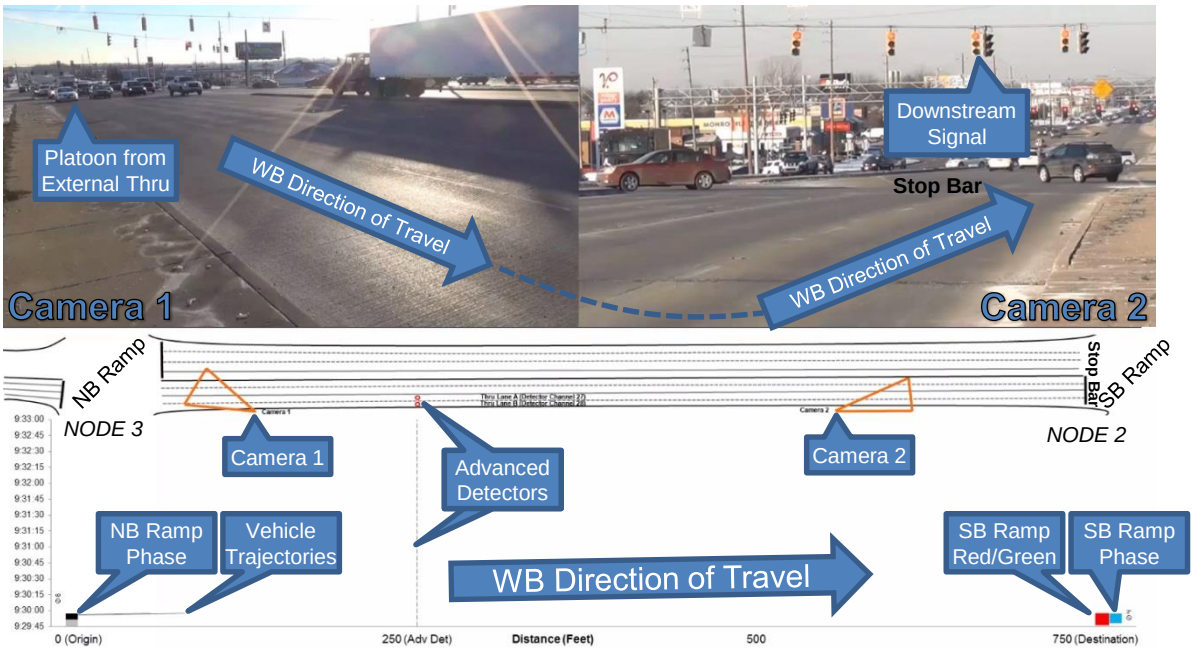

a) Explanation of video layout

b) QR Code for Video **http://dx.doi.org/10.4231/R7VD6WCH**

Figure 12 Video components documenting Westbound traffic operations after optimized lead-lead sequence implemented on December 5, 2013